

## $\beta$ -decay and neutron emission studies of r-process nuclei near $^{137}\text{Sb}$

Karl Smith<sup>\*,1,2,3</sup>, F. Attallah<sup>4</sup>, T. Faestermann<sup>5</sup>, U. Giesen<sup>6</sup>, H. Geissel<sup>4</sup>, M. Hannawald<sup>7</sup>, M. Hausmann<sup>4</sup>, M. Hellström<sup>4</sup>, R. Kessler<sup>7</sup>, K.-L. Kratz<sup>7</sup>, H. Mahmud<sup>8</sup>, Y. Litvinov<sup>4</sup>, M. N. Mineva<sup>9</sup>, F. Montes<sup>1,3</sup>, G. Münzenberg<sup>4</sup>, B. Pfeiffer<sup>7</sup>, J. Pereira Conca<sup>1,3</sup>, P. Santi<sup>10</sup>, H. Schatz<sup>1,2,3</sup>, C. Scheidenberger<sup>4</sup>, K. Schmidt<sup>4</sup>, R. Schneider<sup>5</sup>, A. Stolz<sup>1</sup>, K. Sümmerer<sup>4</sup>, J. Stadlmann<sup>11</sup>, E. Wefers<sup>5</sup>, & P.J. Woods<sup>7</sup>

<sup>1</sup>National Superconducting Cyclotron Laboratory (NSCL)

<sup>2</sup>Dept. of Physics and Astronomy, Michigan State University

<sup>3</sup>The Joint Institute for Nuclear Astrophysics (JINA)

<sup>4</sup>Helmholtzzentrum für Schwerionenforschung (GSI)

<sup>5</sup>TU München

<sup>6</sup>University of Notre Dame

<sup>7</sup>Universität Mainz

<sup>8</sup>University of Edinburgh

<sup>9</sup>Lund University

<sup>10</sup>Los Alamos National Laboratory

<sup>11</sup>Universität Giessen

E-mail: [ksmith@nscl.msu.edu](mailto:ksmith@nscl.msu.edu)

$\beta$ -decay half-lives and neutron emission probabilities ( $P_n$ ) play an important role in r-process nucleosynthesis. An experiment was performed at GSI to measure  $\beta$ -decay half-lives and  $P_n$  values in the  $A=130$  region including the waiting point nuclei  $^{136}\text{Sn}$  and  $^{137}\text{Sb}$ . The experiment was performed with a stack of four 500  $\mu\text{m}$  thick double sided silicon strip detectors along with the Mainz  $4\pi$  neutron long counter detector. The system allows to time correlate ion implant and decay events and the detection of the neutrons emitted during the decay. We discuss the analysis approach and some preliminary results.

*11th Symposium on Nuclei in the Cosmos - NIC XI*  
Heidelberg, Germany  
July 19–23 2010

---

\* Speaker

## 1. Introduction

The rapid neutron capture process, r-process, differs from the slow neutron capture process, s-process, by capturing neutrons on a shorter timescale than the respective  $\beta$ -decay for the target nucleus. The r-process therefore involves formation of nuclei further away from the valley of stability. Since the  $\beta$ -decay timescale is large compared to the neutron capture timescale, the  $\beta$ -decay half-lives determine the speed of the process and the abundance pattern. [1][2][3]

Toward the end of the r-process the neutron abundance drops, and at this point the  $\beta$ -unstable nuclei begin to  $\beta$ -decay back toward stability. There is a finite probability,  $P_n$ , for neutron emission during  $\beta$ -decay if the neutron-separation energy is less than the decay Q-value. Neutron emission will modify the final abundances produced in the r-process by shifting the abundance from an isobar with mass A to one with mass A-1. Neutron emission also impacts the neutron abundance during freezeout. It has been pointed out that neutron emissions smooth out odd-even effects so that the final abundances more closely resemble observed solar r-process abundances [4], though other effects such as late time neutron capture have similar effects.

## 2. Experimental setup

An experiment to measure  $\beta$ -decay half-lives and neutron emission probabilities for nuclei near  $^{137}\text{Sb}$  was performed at the Helmholtzzentrum für Schwerionenforschung (GSI) in Darmstadt, Germany. A primary beam of  $^{238}\text{U}$  originating from the Heavy Ion Synchrotron (SIS) accelerator impinged upon a lead fission target to create a fragment beam of rare isotopes around  $^{137}\text{Sb}$ . Detectors set at the dispersive and focal planes of the Fragment Separator (FRS) [5] were used to identify fragments by energy loss, magnetic rigidity, and time-of-flight. These included a set of Multiwire Proportional Counters (MWPC), a MUSIC detector and a scintillator where position, energy loss and time-of-flight were determined, respectively (Fig. 1).

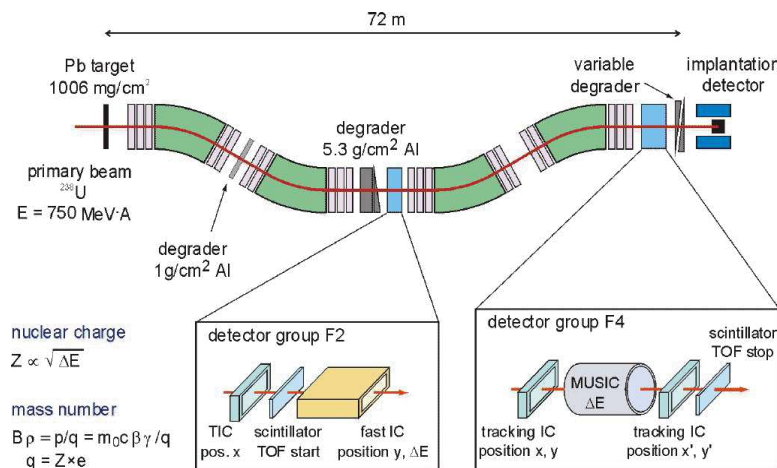


**FIGURE 1:** Illustration of the Fragment Separator (FRS) at GSI including detectors used for particle identification.

After identification of the isotopes the beam was further slowed using a variable degrader such that the isotopes of interest were implanted into a set of detectors used to determine  $\beta$ -decay half-lives and neutron emission probabilities (Fig. 2). The implantation and decay detector consisted of a stack of four double sided 500  $\mu\text{m}$  thick silicon strip detectors (DSSDs).  $\beta$ -particles from the decay of the implanted isotopes were also detected. The Mainz neutron long counter surrounded the DSSD stack for determining the  $P_n$  values. The long counter consists of a set of  $^3\text{He}$  gas proportional counters embedded in a polyethylene matrix to moderate the neutrons for increased detection efficiency.

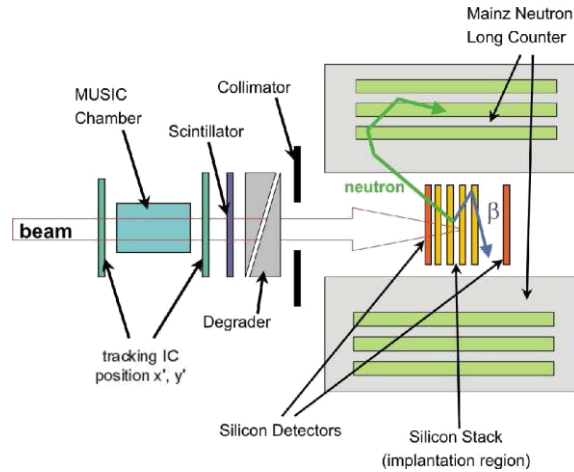


**FIGURE 2:** Illustration of the implantation detectors at the final focal plane of the FRS. The incoming beam is slowed with a variable degrader and then implanted into a stack of silicon detectors. Neutrons emitted in coincidence with  $\beta$ -decays were detected in the surrounding long counter.

Implantation events were correlated with decay events that occurred within ten seconds of each other and within a correlation volume around the location of the implantation. This volume may include  $\beta$ -decays on a detector adjacent to the DSSD in which the isotope was implanted. The volume was selected in such a way to maximize  $\beta$  detection efficiency and to minimize random background correlations.

### 3. Background Subtraction

The resulting decay-time histograms contain random background events. Some of this background is related to a light ion contamination in the secondary beam that deposits little energy when passing through the detector mimicking the behavior of  $\beta$  particles. Most of these light ions leave a straight track through the entire detector stack and can therefore easily be rejected, but owing to the finite detector efficiency some background remains that cannot be distinguished from  $\beta$  particles.

Another complication is that this beam related background has the time structure of the SIS beam, arriving at the detector in spills about one second wide with about a four second separation between spills. In addition, beam intensity during a spill varies as a function of time, and there are also variations from spill to spill. Therefore, the background at the implantation detector had a complex time structure that varied from event to event. [6]

For short half-lives, the decay occurs mostly within a spill, but not always as the implantation can occur towards the end of a spill. We solved this problem by taking advantage of the fact that the time dependence of the background is the same across the detector. For each implantation of the nucleus of interest, we create a virtual implant at another location to determine the background at the same time. The location of the virtual implant is chosen using the probability distribution of the actual implantation location. Therefore, the time structure of the background is accounted for exactly, while the position dependence of the background is accounted for in a statistical sense for the entire ensemble of implanted ions.

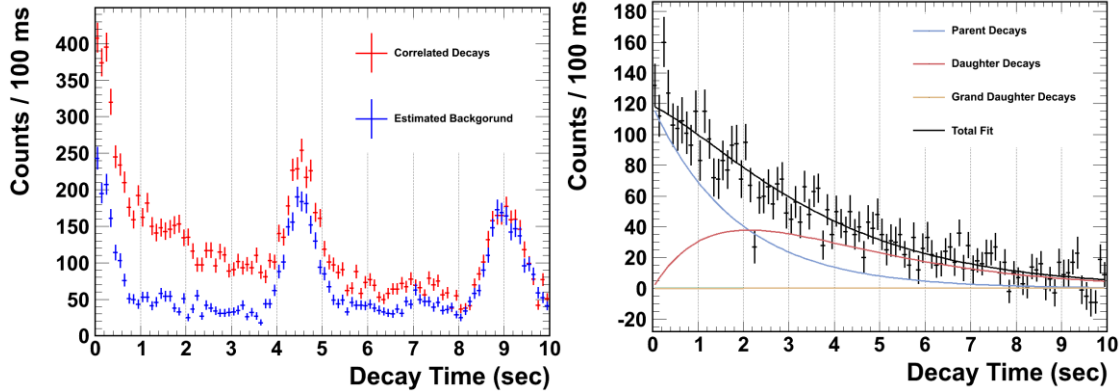


**FIGURE 3:** Total  $\beta$ -decay curve for  $^{142}\text{Xe}$  (left, red) shows a dependence on the structure of the beam produced by the SIS. Spills have a width of about one second with a four second spill separation. The calculated background for  $^{142}\text{Xe}$  (blue) is also shown. The right figures shows the background subtracted total  $\beta$ -decay curve for  $^{142}\text{Xe}$  and the fit used to determine half-life and parent decays (parent decays in blue and daughter decays in red).

The correlation that was used for the real implantations was then repeated using the virtual implant. The events correlated to the virtual implant must then be background events since they occurred in another region of the DSSDs without a real implant associated with it. A background histogram was then created and subtracted from the histogram of the correlated decay times. The resulting decay curve is background free and was fitted with the parent half-life and the efficiency as free parameters. Error bars were determined by propagation taking into account the background subtraction procedure.

Neutron emission probabilities were determined by the ratio of all parent  $\beta$ -decay events as determined by the decay curve fit, and the subset of such events with a detection of a neutron. Preliminary results show antimony isotopes,  $^{134}\text{Sb}$ [7][8][9],  $^{135}\text{Sb}$ [8][10][11][12][13],  $^{136}\text{Sb}$ [8],  $^{137}\text{Sb}$ [13], agreeing with previously published results. This work will include first time measurements of half-lives and  $P_n$  values for  $^{138-139}\text{Sb}$ ,  $^{139-141}\text{Te}$ , and  $^{143}\text{I}$ .

#### 4. Acknowledgements

Work supported in part by National Science Foundation Grant PHY-06-06007 (NSCL) and PHY 08-22648 (Joint Institute for Nuclear Astrophysics).

## References

- [1] E. M. Burbidge et al., *Synthesis of the Elements in Stars*. Rev. Mod. Phys. **29**, 547 (1957)
- [2] J. J. Cowan, F.-K. Thielemann, and J. W. Truran, *The R-process and nucleochronology*. Phys. Rep. **208**, 267 (1991)
- [3] M. Arnould, S. Goriely, and K. Takahashi, *The r-process of stellar nucleosynthesis: Astrophysics and nuclear physics achievements and mysteries*. Phys. Rep. **450**, 97 (2007)
- [4] K. Kratz et al., *Isotopic r-process abundances and nuclear structure far from stability implications for the r-process mechanism*. ApJ **403**, 216-238 (1993)
- [5] H. Geissel et al., *The GSI projectile fragment separator (FRS): a versatile magnetic system for relativistic heavy ions*. Nucl. Instrum. Methods B **70**, 286 (1992)
- [6] T. Kurtukian-Nieto, J. Benlliure and K.-H. Schmidt, *A new analysis method to determine  $\beta$ -decay half-lives in experiments with complex background*. Nucl. Instrum. Methods A **589**, 472 (2008)
- [7] A. Kerek, et al., *Two-proton and proton-neutron states in the doubly closed shell  ${}_{50}^{132}\text{Sb}_{81}\text{Sn}_{82}$  region*. Nucl. Phys. A **195**, 177 (1972)
- [8] B. Fogelberg, et al., *Decays of  ${}^{134}\text{Sn}$  and  ${}^{134}\text{Sb}$* . Phys. Rev. C **41**, 1890 (1990)
- [9] G. Rudstam, K. Aleklett, and L. Sihver., *Delayed-Neutron Branching Ratios of Precursors in the Fission Product Region*. At. Data Nucl. Data Tables **53**, 1 (1993)
- [10] L. Tomlinson, and M.H. Hurdus., *Delayed neutron precursors-II: Antimony and arsenic precursors separated chemically*. Journal of Inorganic and Nucl. Chem. **30**, 1649 (1968)
- [11] L. Tomlinson, and M.H. Hurdus., *Delayed neutron precursors-I: Antimony and arsenic precursors separated by electrolysis*. Journal of Inorganic and Nucl. Chem. **30**, 1125 (1968)
- [12] W. Rudolph, K.-L. Kratz, and G. Herrmann., *Half-lives, fission yields and neutron emission probabilities of neutron-rich antimony isotopes*. Journal of Inorganic and Nucl. Chem. **39**, 753 (1977)
- [13] J. Shergur et al.,  *$\beta$ -decay studies of  ${}^{135-137}\text{Sn}$  using selective resonance laser ionization techniques*. Phys. Rev. C **65**, 034313 (2002)